

## EXPERIMENTAL STUDY ON THE EFFECT OF A DEFORMABLE BOUNDARY ON THE COLLAPSE CHARACTERISTICS OF A CAVITATION BUBBLE

by

**Yanwei ZHAI\***, Weilin XU, Jing LUO, and Qi ZHANG

State Key Laboratory of Hydraulics and Mountain River Engineering,  
Sichuan University, Chengdu, China

Original scientific paper  
<https://doi.org/10.2298/TSCI1904195Z>

*Cavitation phenomena widely exist in many fields such as medical treatment, chemical engineering, and hydraulic engineering. The boundary properties have a great influence on the collapse characteristics of a cavitation bubble. The interaction between a cavitation bubble and a boundary of different properties is an important part in the cavitation erosion mechanism. In this paper, cavitation bubbles under in-water pulse discharge and cavitation erosion under ultrasonic vibration were used to study the effect of a deformable boundary on the collapse characteristics of a cavitation bubble, which reveals the cavitation-resistance performance of different materials on the macroscopic scale. The main experimental results showed that on a deformable boundary, the cavitation bubble does not collapse toward the boundary in the later collapse stage compared with on the rigid boundary. The collapse process of the cavitation bubble is aggravated on the deformable boundary. In the condition of same cavitation strength, the cavitation's erosion loss amount on the rigid boundary material is much higher than that on the deformable boundary material. The experimental conclusions have an important reference value for the development of cavitation erosion prevention and the exploration of cavitation-resistance materials.*

Key words: *cavitation bubble, micro-jet, deformable boundary, cavitation erosion, collapse characteristics, bubble electrospinning*

### Introduction

Cavitation phenomena widely exist in many fields such as medical treatment, chemical engineering, and hydraulic engineering. However, this phenomenon in hydraulic engineering needs to be avoided as soon as possible [1-3]. When the liquid at a constant pressure is heated or the liquid at a constant temperature is decompressed by a static or dynamic method, there are steam bubbles or cavitation bubbles filled with steam under certain conditions, which called cavitation phenomenon. When the collapse of cavitation bubbles occurs within a certain distance from boundary surface, the solid wall surface will be subjected to impact effect that results in boundary material erosion or fatigue damage and fracture. Therefore, the interaction between a cavitation bubble and a wall surface has always been an important part of cavitation effect researches.

---

\* Corresponding author, e-mail: zhaiyw1992@163.com

At present, many scholars have studied the interaction between cavitation bubbles and a free water surface or a rigid boundary. The cavitation bubble dynamics were classified by Plesset and Prosperetti [4]. Xu *et al.* [5] experimentally studied the movement relationship between a cavitation bubble and an air bubble near a rigid boundary, obtained the critical conditions to change the collapse direction of the cavitation bubble, and revealed the vector synthesis mechanism among above three factor interaction. Luo *et al.* [6] studied a cavitation bubble and an air bubble, and interaction between two cavitation bubbles. Found that the air bubble could affect the cavitation bubble evolution period and the collapse direction among multiple cavitation bubbles. Zhang *et al.* [7] studied the interaction between a cavitation bubble and a free water surface, and obtained the collapse direction of the cavitation bubble under the free surface.

The interaction between cavitation bubbles and deformable boundaries has attracted much attention for many years. With schlieren photography and Mach-Zehnder interferometry techniques, Shaw *et al.* [8] presented a sequence of schlieren images of the evolution of a laser generated cavitation bubble created in-water near the inertial boundary, followed by the corresponding interferometry sequence. Sankin and Zhong [9] measured the impact of cavitation bubbles near a silicone rubber membrane and discussed the influencing factors of impact force. Brujan *et al.* [10] and Vogel *et al.* [11] studied the interaction between cavitation bubble and elastic boundary, and their dependence on the distance between the bubble and the boundary. It was considered that the micro-jet was caused by the interaction of reaction force caused by the rebound on the elastic boundary and the Bjerknes attraction force to the boundary. Gibson and Black [12] experimented with several different surface coatings, believed that the form of cavitation bubble collapse near the boundary can be described by inertia and stiffness. Shima *et al.* [13] and Tomita and Kodama [14] observed similar phenomena in experiments, found that bubble migration depends on its size and the distance from the bubble to the boundary surface. Duncan and Zhang [15] and Duncan *et al.* [16] simulated numerically similar cases to the experiments and modeled coating material as a spring foundation with parameters such as spring mass, spring stiffness and coating radius. Their simulation results were qualitatively consistent with the experimental data. Goh *et al.* [17] investigated interaction between a spark-generated bubble and an elastic sphere. The simulation results were in accordance with the experimental data. The numerical model was then extended to study the effects of elasticity and experimental parameters. Gong *et al.* [18] studied the interaction between a spark-generated bubble and a two-layered composite beam. Both numerical and experimental approaches were employed to investigate the dynamics of bubble collapse near the two-layered composite beam, which revealed that the bubble collapse time is greatly influenced by the nearby two-layered composite beam.

Previous studies using experiments or numerical simulation, most studies were based on a rigid wall or an elastic membrane. There were a few studies on the collapse characteristics of a cavitation bubble near a boundary with deformable materials and the effects of cavitation bubble collapse on the erosion of boundary materials. Therefore, the paper studied the collapse process of different size cavitation bubbles near the boundary, and analyzed their collapse direction and evolution period, by in-water pulse discharge technology to induce a cavitation bubble and high-speed photography. The erosion characteristics of the boundary materials were observed and analyzed through above experiments and the ultrasonic vibration cavitation experiments. The conclusions can provide a reference for the development of the cavitation erosion prevention and the exploration of the cavitation-resistance materials.

## Experimental equipment and method

### Experimental equipment

The experimental system to induce a cavitation bubble with in-water pulse discharge was shown in fig. 1(a). The 220 V AC power was boosted by a transformer and rectified by a silicon stack to the DC, which could reach a maximum of 30 kV. Then the charge energy was stored in a capacitor of 500 kV and 0.25  $\mu$ F. When the electric quantity stored in the capacitor reached a certain value, water body between the electrodes placed into a tank could be punctured, and the breakdown energy could induce a cavitation bubble at the center of the electrodes. By adjusting the value of the resistor, the discharge intensity was varied with controlling the discharge pulse width, so that the size of a cavitation bubble was changed. Due to the very short time and smaller scale of cavitation bubbles growth and collapse, the high-speed camera recording system with Fastcam SA-Z was used for photography, whose type of the lens was Nikon IF Aspherical Macro. For the high-speed dynamic acquisition and analysis system, demand on the lighting conditions of shooting environment was very strictly. Therefore, it was necessary to use a cold light source with extremely low calorific power as a light-filling device during the experiment. It was necessary to verify the mesoscopic mechanism of the interaction between a cavitation bubble and a deformable boundary by the macroscopic erosion experiments of ultrasonic cavitation. The test system of ultrasonic vibration cavitation included an ultrasonic generator, a piezoelectric ultrasonic transducer, a horn, and a beaker, as shown in fig. 1(b). The system was based on the principle presented in ASTM G32-16. The frequency and power of the experimental equipment were 10-100 KHz and 0-500 W, respectively.

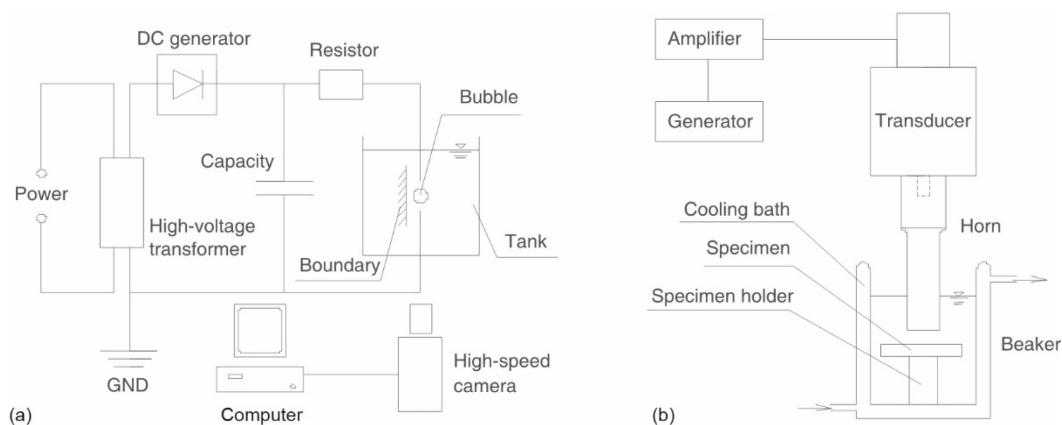


**Figure 1. Diagram of the experimental equipment; (a) the experimental system to induce a cavitation bubble with in-water pulse discharge, (b) the test system of ultrasonic vibration cavitation**

### Experimental method

Since the cavitation bubble was quite sensitive to the outside temperature and pressure environment, the microscopic interaction between a cavitation bubble and a deformable boundary had to be conducted in a constant temperature and pressure environment. The atmospheric pressure and in-water temperature of the experimental tank were 94.77 kPa and  $25 \pm 2$   $^{\circ}$ C, respectively. The discharge electrodes in-water were placed in a transparent glass

tank with length  $\times$  width  $\times$  height of 400 mm  $\times$  150 mm  $\times$  250 mm. Secondary deionized water containing extremely low impurities and gas nucleus was used in the experiment, whose liquid level in the tank was 200 mm. The electrodes were located in 100 mm below the water top surface. The positions of the electrodes and boundary material were shown in fig. 1(a). The material of deformable boundary was made of silicone rubber in line with relevant specifications and had well hydrophobicity and stability. The rigid boundary material was made of 304 stainless steel, whose surface was treated with mirror polishing. The mechanical properties of boundary materials were shown in tab. 1. The whole processing of the growth and collapse of cavitation bubbles were photographed and recorded with the high-speed camera in the experiments. In order to simplify the research, the dimensionless distance from the center of the cavitation bubble to the boundary  $\gamma$  was defined:

$$\gamma = \frac{D}{R_{\max}} \quad (1)$$

where  $\gamma$  is the dimensionless distance from the cavitation bubble to the boundary,  $D$  [mm] – the distance from the center of the cavitation bubble to the boundary, and  $R_{\max}$  [mm] – the maximum radius of the cavitation bubble.

**Table 1. Parameters of experimental boundary materials**

Materials	Silicone rubber	304 stainless steel
Size (length $\times$ width $\times$ thickness) [mm]	30 $\times$ 30 $\times$ 10	30 $\times$ 30 $\times$ 10
Tensile modulus [MPa]	0.13	29000
Youngs modulus [MPa]	0.50	193000

The cavitation erosion experiments at the macroscopic level were carried out by ultrasonically induced cavitation bubble cloud in different properties of boundary materials. The beaker liquid level was 100.0  $\pm$  2.0 mm with the medium of deionized water. The temperature of experimental water was controlled at constant 25  $\pm$  2  $^{\circ}$ C by the circulating water cooling system. The specimens of boundary materials were fixed below the radiating surface of the horn at a spacing of 5.0  $\pm$  0.1 mm. The working frequency and setting power of ultrasonic transducer operated were 20.0  $\pm$  0.2 KHz and 100 W, respectively. The cumulative experimental time was 4.5 hours. The specimens were removed every 0.5 hours. After alcohol cleaned, constant temperature dried, and placed one day in the drier, the specimens were weighed by the analytical balance with an accuracy of 0.01 mg. Every specimens were weighed five times and their average weighting were taken as their weights. Therefore, the curves of cumulative erosion loss amount and erosion loss rate of the specimens were drawn out.

### Results analysis

While a cavitation bubble collapsed within a certain distance from a rigid boundary, the boundary would be impacted by the shock wave and micro-jet of bubble collapse, which resulted in cavitation erosion of the boundary material. Collapse direction of a cavitation bubble represented micro-jet direction. From collapse direction of a cavitation bubble, it could be judged whether there was a micro-jet impact on the boundary. The energy release rate of a cavitation bubble was reflected by its evolution time. By means of the high-speed photog-

raphy, collapse direction and evolution time of the bubble were observed during the interaction between the bubble and deformable boundary, which showed the mesoscopic mechanism of cavitation bubble collapse on the boundary. Through the above mesoscopic researches, the macroscopic characteristics of material erosion could be revealed.

*Boundary effect on the direction of the cavitation bubble collapse*

Changing the size of cavitation bubbles and the distance from the center of the cavitation bubble to the boundary, the dimensionless distance,  $\gamma$ , could be controlled at 0.79-1.81.

Figure 2 showed a cavitation bubble collapse process and the strong wall effect near the rigid boundary. The surrounding waterbody would quickly fill in the gap created by cavitation bubble contraction when the cavitation bubble reached the maximum volume shown in fig. 2(a) and entered the contraction phase. For the rigid boundary, the waterbody rate between the cavitation bubble and the boundary toward the bubble center was slower than that far from the boundary, fig. 2(b). The movement rate of cavitation bubble surface far from the boundary was faster than that near the boundary, fig. 2(c). Micro-jet pointing to the boundary was generated away from the boundary, fig. 2(d). The micro-jet pierced the bubble surface and stroked the rigid boundary at the final collapse stage, figs. 2(e) and 2(f), then the first collapse time was completed. The second collapse time of the cavitation bubble occurred directly on the rigid boundary, and the cavitation bubble rebounded on the boundary, figs. 2(g) and 2(h).

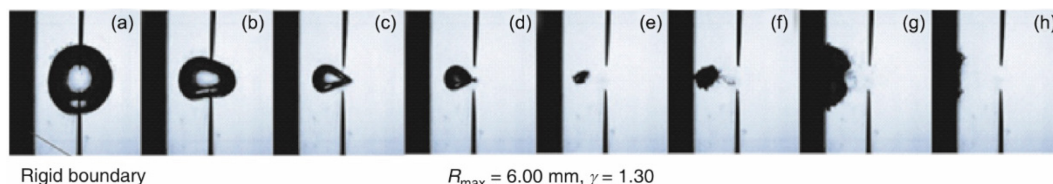


**Figure 2. Cavitation bubble collapse process near the rigid boundary**  
 (frame rate: 200 000 fps, exposure time: 5  $\mu$ s)

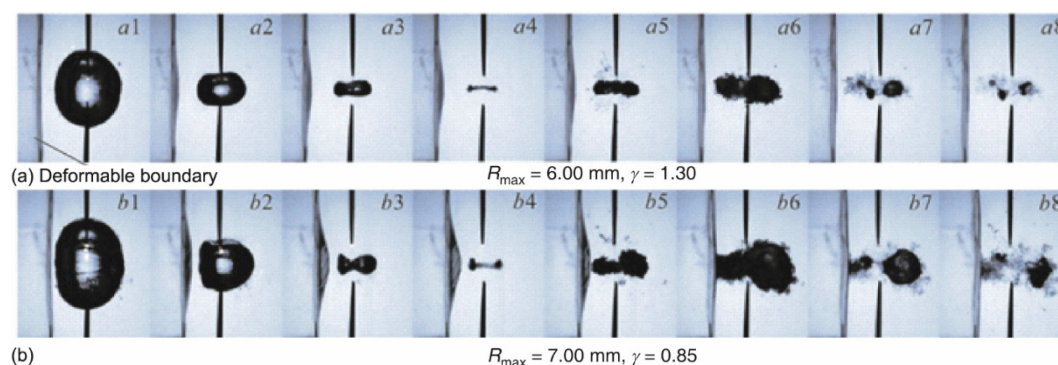


**Figure 3. Cavitation bubble collapse process near the deformable boundary**  
 (frame rate: 200 000 fps, exposure time: 5  $\mu$ s)

Figure 3 showed the collapse process of a cavitation bubble near the deformable boundary. In experiment group A, the maximum radius of the cavitation bubble was 6.00 mm, the dimensionless distance,  $\gamma$ , was 1.30. In experiment group b, the maximum ra-

dius of the cavitation bubble was 7.00 mm, the dimensionless distance,  $\gamma$ , was 0.85. In the first collapse period of cavitation bubble, there was no movement towards the boundary (showed as *a1-a4*, *b1-b4* in fig. 3). The shape of the cavitation bubble was relatively symmetrical, and micro-jet did not occur obviously. The boundary material gradually bulged during this process. While the dimensionless distance was smaller, the boundary material bulged was more obviously (*b5*). When the cavitation bubble evolved to the second stage, the boundary material was gradually restored to the plane (*a6*, *b6*) along with the second expansion of the cavitation bubble. Since then, the cavitation bubble was gradually dissipated and no longer had a significant effect on the boundary (*a7* and *a8*, *b7* and *b8*).

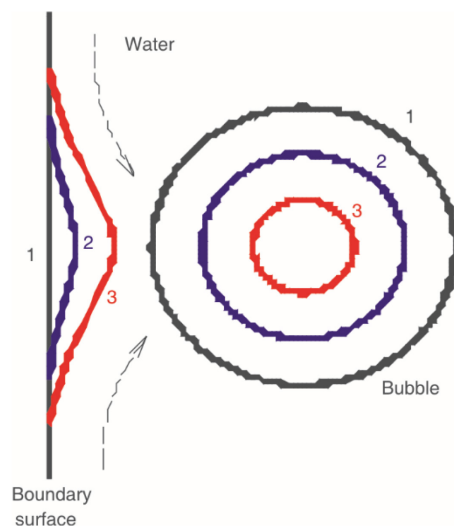


**Figure 4.** Interaction schematic between a cavitation bubble and a deformable boundary

As shown in fig. 4, the effect of the cavitation bubble on the boundary material mainly happened during the first collapse time. When the cavitation bubble reached the maximum volume, the deformable boundary was in the original state (1). With the shrinkage of the cavitation bubble, the waterbody near the boundary was blocked on the boundary while the surrounding waterbody flowed back into the gap, so that the backflow was less than that on the non-boundary side. The surface of the deformable boundary material was gradually bulged, which filled up the gap of the waterbody near the boundary to a certain degree, so that the cavitation bubble had a more symmetrical shape during its contraction process, and there was no micro-jet (2). In the cavitation bubble collapse stage, the boundary bulge reached the maximum amount (3).

The collapse pattern and direction of the cavitation bubbles were distinctly different on a rigid boundary from that on a deformable boundary. The reasons for this phenomenon were as follows: under the influence of the rigid boundary, in the cavitation bubble collapse stage, the waterbody near the boundary surface was blocked by the rigid boundary. While the waterbody far from the boundary belonged to unbounded domain that led to the asymmetry of cavitation contraction process. Therefore, shrinkage rate of the cavitation bubble surface far from the boundary was larger than that near the boundary. Finally, a micro-jet was formed and directly impacted on the boundary. Since the deformable boundary material was more elasticity, the block of the waterbody backflow was weakened to a certain extent. Then the asymmetry of bubble contraction process was also weakened. Therefore, there was no tendency for the center of the cavitation bubble to move toward boundary surface, and no obvious micro-jet.

#### *Boundary influence on evolution period of cavitation bubbles*

Collected by the high-speed camera, the photographs were transposed into grayscale images to distinguish the number of pixels occupied by cavitation bubbles corresponding to the grayscale range. Combined with the actual size of the pixel calibration, cavitation bubble radius changing with the time could be obtained during the evolution of

cavitation bubble. The curves in fig. 5 were derived from the evolution of cavitation bubbles in figs. 2 and 3(a). With the same  $R_{max}$ , the first collapse period of the cavitation bubble near the deformable boundary was 1155  $\mu$ s, and the second collapse period was 550  $\mu$ s. While the first collapse period of the cavitation bubble near the rigid boundary was 1275  $\mu$ s, and the second collapse period was 900  $\mu$ s. Therefore, the collapse time of cavitation bubble near the deformable boundary was shorter than that near the rigid boundary. The first collapse period was shortened by 9% and the second collapse period was 40%. The minimum radius of the cavitation bubble collapse near the deformable boundary was 1.17 mm, while those near the rigid boundary was 1.24 mm. Both above minimum radiuses were closer. The collapse period of the cavitation bubble near the deformable boundary was shorter, and the rate of expansion and contraction of the cavitation bubble surface near the deformable boundary was faster than that near the rigid boundary. The relationship between collapse time in the first period and the maximum radius of different bubbles was obtained by changing the size of cavitation bubbles, as shown in fig. 6. The evolution period of cavitation bubbles near the deformable boundary was shorter than that near the rigid boundary. It can be seen from the regression curves that when the  $R_{max}$  was smaller, the evolution period of cavitation bubbles had less difference, and the differences in evolution period of cavitation bubbles increased with the  $R_{max}$  gradually increasing.

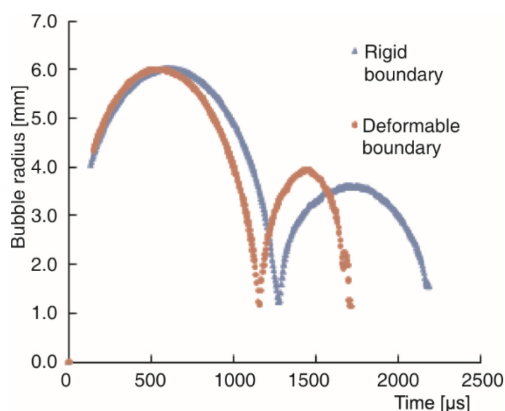


**Figure 5. Radius of cavitation bubbles with their evolution time**

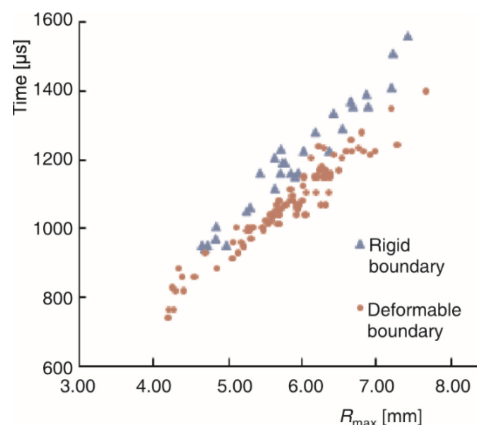


**Figure 6. Relationship between the maximum radiuses of cavitation bubbles and their collapse time in the first period**

The cavitation bubble evolution period showed the waterbody blocked on the rigid boundary, and reduced the expansion and contraction process of cavitation bubble surface. Especially in the second collapse period, the evolution period of the cavitation bubble surface on the rigid boundary was further increased. The deformable boundary had less blocked effect on the waterbody and less influence on the expansion and contraction process of the cavitation bubble surface. The shorter the cavitation bubble collapse period was, the stronger the shock wave or micro-jet would be at the cavitation bubble collapse. Although there was no movement towards the boundary while the cavitation bubble collapsed near the deformable boundary, collapse period was shorter and the shock wave generated by the cavitation bubble collapse might affect on boundary materials.

### *Cavitation erosion characteristics of the deformable boundary material*

From the mesoscopic analysis, it can be seen that, although cavitation bubbles near the deformable boundary were not moving towards the boundary during their collapse process, a large deformation occurred on the boundary material, and the cavitation bubble collapse period was shorter. For the deformable boundary material, with cavitation cloud generated by ultrasonic waves inducing direct action, cavitation erosion characteristics could be studied from the macroscopic level.

The relationship between cumulative erosion loss amount (CELA) and erosion time on boundary materials was shown in fig. 7. At first, CELA on the rigid boundary material increased slowly in the experiment, then increased uniformly after 1.5 hours. Final total CELA was 72.60 mg. The CELA on the deformable boundary material was far less than that on the rigid one, the change process was more uniform, and total CELA was only 11.90 mg.

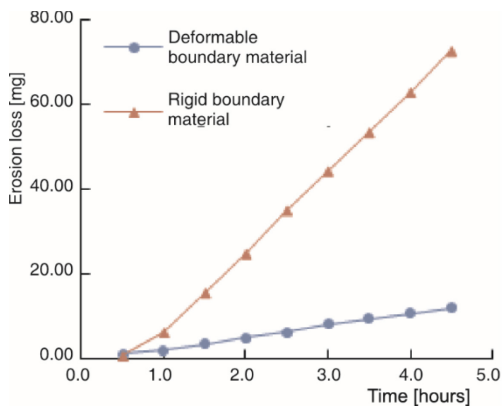


Figure 7. The CELA vs. time

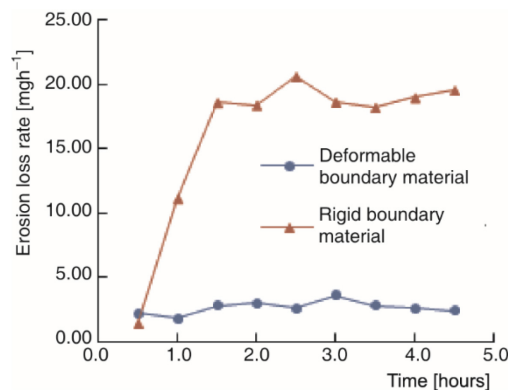


Figure 8. Erosion loss rate vs. time

The relationship between erosion loss rate and erosion time was shown in fig. 8. Erosion loss rate of the rigid boundary material changed greatly, which increased gradually from 1.40 mg/h at the beginning to 18.58 mg/h. Erosion loss rate on the rigid boundary material was divided into three stages: incubation stage, acceleration stage and stabilization stage. At the beginning of the experiment, the surface of the rigid boundary material was smooth and flat, and the resistance to cavitation erosion was better, which was the incubation stage. With the cavitation evolution, cavitation pits began to occur, and the surface of the rigid boundary material became rough as numbers of cavitation pits gradually increased, and the erosion loss rate increased also (0.5-1.5 hours), which was the acceleration stage. With the further action of cavitation, the surface roughness was relatively stable and the erosion loss rate was stable (1.5-4.5 hours), which was the stabilization stage. Initially the erosion loss rate of the deformable boundary material was lower, only 2.20 mg/h. Then there was no obvious acceleration or inflection point and the erosion loss rate remained lower. The material surface of the deformable boundary after the experiment was as smooth as it before experiment without a pit or breakage. The natural weight loss of deformable boundary material was about 1.00 mg per day when it was placed in the air. The experimental time interval was one day, and CELA in the experiment to 9<sup>th</sup> day was 11.90 mg. The CELA of the deformable boundary material was essentially a systematic error caused by the natural weight loss of the material itself,

and there was no obvious cavitation phenomenon on the deformable boundary material. Therefore, CELA of the deformable boundary material was still much smaller, even if the boundary material was under the long-term action of cavitation cloud.

## Conclusions

Through the experiments of a cavitation bubble induced by in-water pulse discharge and ultrasonic vibration cavitation erosion, the effect of the deformable boundary on the collapse characteristics of the cavitation bubble was studied from mesoscopic level, which revealed macroscopic cavitation erosion resistance of different materials. The experimental conclusions are shown as follows.

- The boundary characteristics have a great impact on the collapse direction of the cavitation bubble. Under the effect of the deformable boundary, the cavitation bubble does not collapse toward the boundary in the later collapse stage compared with the rigid boundary. There are obvious stretching and compression phenomena on the deformable boundary during the evolution of the cavitation bubble.
- Under the conditions of same feature parameters of cavitation bubbles, duration time in the expansion stage of cavitation bubbles influenced on the deformable boundary is equivalent to that on the rigid boundary, while duration time in the contraction stage is affected by the deformable boundary, *i. e.* the deformable boundary aggravates the collapse process of cavitation bubbles.
- Under the conditions of same cavitation strength, cavitation erosion loss amount on the rigid boundary material is much higher than that on the deformable boundary material.
- The present results are also helpful to design an optimal bubble electrospinning setup for fabrication of nanofibers [19-21].

## Acknowledgment

This work was supported by the National Key R&D Program of China (Grant No.2016YFC0401901) and Postdoctoral R&D Program of Sichuan University (Grant No. 2018SCU12061).

## References

- [1] Hutli, E., et al., Appearance of High Submerged Cavitating Jet: the Cavitation Phenomenon and Sono Luminescence, *Thermal Science*, 17 (2013), 4, pp. 1151-1161
- [2] Zhang, D. S., et al., Numerical Investigation of Time-Dependent Cloud Cavitating Flow around a Hydrofoil, *Thermal Science*, 20 (2016), 3, pp. 913-920
- [3] Krefting, D., et al., High-Speed Observation of Acoustic Cavitation Erosion in Multibubble Systems, *Ultrasonics Sonochemistry*, 11 (2004), 3-4, pp. 119-123
- [4] Plesset, M. S., Prosperetti, A., Bubble Dynamics and Cavitation, *Annual Review of Fluid Mechanics*, 9 (1977), 1, pp. 145-185
- [5] Xu, W. L., et al., Interaction of a Cavitation Bubble and an Air Bubble with a Rigid Boundary, *J. Hydrodyn.*, 22 (2010), 4, pp. 503-512
- [6] Luo, J., et al., Experimental Study of the Interaction between the Spark-Induced Cavitation Bubble and the Air Bubble, *J. Hydrodyn. Ser. B*, 25 (2013), 6, pp. 895-902
- [7] Zhang, A. M., et al., Experiments on Bubble Dynamics between a Free Surface and a Rigid Wall, *Exp. Fluids*, 54 (2013), 10, pp. 1602
- [8] Shaw, S. J., et al., Experimental Observations of the Interaction of a Laser Generated Cavitation Bubble with a Flexible Membrane, *Phys. Fluids*, 11 (1999), 8, pp. 2437-2439
- [9] Sankin, G. N., Zhong, P., Interaction between Shock Wave and Single Inertial Bubbles near an Elastic Boundary, *Phys. Rev. E - Stat. Nonlinear, Soft Matter Phys.*, 74 (2006), 4 Pt 2, pp. 046304

- [10] Brujan, E. A., et al., Dynamics of Laser-Induced Cavitation Bubbles near an Elastic Boundary Used as a Tissue Phantom, *J. Fluid Mech.*, 433 (2001), March, pp. 251-281
- [11] Vogel, A., et al., Interaction of Laser-Produced Cavitation Bubbles with Elastic Boundaries, *Proceedings of SPIE - The International Society for Optical Engineering*, 4257 (2001), 1, pp. 381-384
- [12] Gibson, D. C., Blake, J. R., The Growth and Collapse of Bubbles near Deformable Surfaces, *Appl. Sci. Res.*, 38 (1982), 1, pp. 215-224
- [13] Shima, A., et al., The Growth and Collapse of Cavitation Bubbles near Composite Surfaces, *J. Fluid Mech.*, 203 (2006), June, pp. 199-214
- [14] Tomita, Y., Kodama, T., Interaction of Laser-Induced Cavitation Bubbles with Composite Surfaces, *J. Appl. Phys.*, 94 (2003), 5, pp. 2809-2816
- [15] Duncan, J. H., Zhang, S., On the Interaction of a Collapsing Cavity and a Compliant Wall, *J. Fluid Mech.*, 226 (2006), Apr., pp. 401-423
- [16] Duncan, J. H., et al., On the Interaction between a Bubble and a Submerged Compliant Structure, *J. Sound Vib.*, 197 (1996), 1, pp. 17-44
- [17] Goh, B. H. T., et al., Spark-Generated Bubble near an Elastic Sphere, *Int. J. Multiph. Flow*, 90 (2017), Apr., pp. 156-166
- [18] Gong, S. W., et al., Interaction of a Spark-Generated Bubble with a Two-Layered Composite Beam, *J. Fluids Struct.*, 76 (2018), Jan., pp. 336-348
- [19] Yu, D. N., et al., Snail-Based Nanofibers, *Mater. Lett.*, 220 (2018), June, pp. 5-7
- [20] Tian, D., et al., Strength of Bubble Walls and the Hall-Petch Effect in Bubble-Spinning, *Textile Research Journal*, 89 (2018), Apr., pp. 1340-1344
- [21] Sun, Q.-L., et al., Nanoscale Multi-Phase Flow and its Application to Control Nanofiber Diameter, *Thermal Science*, 22 (2018), 1A, pp. 47-50